Non-invasive Dual-Channel Broadband Diffuse Optical Spectroscopy of Massive Hemorrhage and Resuscitative Endovascular Balloon Occlusion of the Aorta (REBOA) in Swine

Jesse H. Lam, BS; Thomas D. O'Sullivan, PhD†; Tim S. Park, MD‡; Jae H. Choi, PhD‡; Robert V. Warren, MS*; Wen-Pin Chen, MS§; Christine E. McLaren, PhD§; COL, MC, US Army Leopoldo C. Cancio, MD‡; Andriy I. Batchinsky, MD‡; Bruce J. Tromberg, PhD**

ABSTRACT Objective: To quantitatively measure tissue composition and hemodynamics during resuscitative endovascular balloon occlusion of the aorta (REBOA) in two tissue compartments using non-invasive two-channel broadband diffuse optical spectroscopy (DOS). Methods: Tissue concentrations of oxy- and deoxyhemoglobin (HbO_2 and HbR), water, and lipid were measured in a porcine model ($n = 10$) of massive hemorrhage (65% total blood volume over 1 h) and 30-min REBOA superior and inferior to the aortic balloon. Results: After hemorrhage, hemoglobin oxygen saturation ($StO_2 = HbO_2/[HbO_2 + HbR]$) at both sites decreased significantly (−29.9% and −42.3%, respectively). The DOS measurements correlated with mean arterial pressure (MAP) ($R^2 = 0.79$, $R^2 = 0.88$), stroke volume (SV) ($R^2 = 0.68$, $R^2 = 0.88$), and heart rate (HR) ($R^2 = 0.72$, $R^2 = 0.88$). During REBOA, inferior StO_2 continued to decline while superior StO_2 peaked 12 min after REBOA before decreasing again. Inferior DOS parameters did not associate with MAP, SV, or HR during REBOA. Conclusions: Dual-channel regional tissue DOS measurements can be used to non-invasively track the formation of hemodynamically distinct tissue compartments during hemorrhage and REBOA. Conventional systemic measures MAP, HR, and SV are uncorrelated with tissue status in inferior (downstream) sites. Multi-compartment DOS may provide a more complete picture of the efficacy of REBOA and similar resuscitation procedures.

INTRODUCTION

Resuscitative endovascular balloon occlusion of the aorta (REBOA) is an emergency resuscitation medical procedure applied in the treatment of severe, non-compressible hemorrhage.[1,2] Although initially explored in the 1950s during the Korean War, the procedure has recently regained international interest in both the military and the civilian sectors.[3–7] The REBOA is a minimally invasive alternative to thoracotomy with aortic clamping, an invasive surgical procedure requiring direct access to the aorta.[2,8] The primary rationale behind REBOA is to induce aortic occlusion using an endovascular balloon in order to stop or slow the rate of uncontrollable hemorrhage.[2] In general, a REBOA device is guided up the femoral artery of a patient and then inflated in the aorta. The induced occlusion restores potentially lifesaving perfusion to the heart and brain, slows the rate of hemorrhage, and ultimately provides medical practitioners more time to stabilize the patient.[9]

Although REBOA is an emerging non-transfusion-based resuscitation technique, assessment of the "two-compartment" REBOA hemodynamics and its effect on tissue oxygenation ($StO_2 = HbO_2/[HbO_2 + HbR]$) and metabolism has yet to be quantified. More specifically, the inflation of an aortic balloon essentially separates the body into two blood volume compartments: (1) upstream from the aortic occlusion, in which blood pressure is restored to critical organs necessary to prolong life and (2) downstream from the aortic occlusion. Clinical measures obtained invasively, such as mean arterial pressure (MAP) and stroke volume (SV), do not provide complete information about StO_2 and metabolism in these two compartments, and they may be inconvenient to use in emergency settings. In contrast, non-invasive broadband diffuse optical spectroscopy (DOS) quickly and easily extracts hemodynamic information based on subsurface tissue chromophore concentrations at multiple sensor locations. Thus, multichannel DOS provides a non-invasive, continuous, and quantitative solution to understand hemodynamics and monitor the effectiveness of REBOA.

*Laser Microbeam and Medical Program, Beckman Laser Institute and Medical Clinic, University of California, Irvine, 1002 Health Sciences Road, Irvine, CA 92617.

†Department of Electrical Engineering, University of Notre Dame, 275 Fitzpatrick Hall, Notre Dame, IN 46556.

‡US Army Institute of Surgical Research, 3698 Chambers Pass STE B JBSA FT Sam Houston, TX 78234.

§Biostatistics Shared Resource, Chao Family Comprehensive Cancer Center, School of Medicine, University of California, Irvine, 101 The City Drive Bldg. 23 Route 81 Orange, CA 92868.

B.J. Tromberg reports patents, which are owned by the University of California, that are related to the technology and analysis methods described in this study. The University of California has licensed diffuse optical spectroscopic imaging technology and analysis methods to Infinit, Inc. This research was completed without Infinit Inc. participation, knowledge, or financial support and data were acquired and processed by coauthors unaffiliated with this entity. The Conflict of Interest: Office of the University of California, Irvine, has reviewed both patent and corporate disclosures and did not find any concerns. No potential conflicts of interest were disclosed by the other authors.

doi: 10.1093/milmed/usx163

The DOS technology employed in this study utilizes a combination of four intensity-modulated lasers and continuous wave (CW) broadband light to quantitatively measure tissue near-infrared absorption and reduced scattering spectra spanning from 650 to 1,000 nm.[10,11] Tissue concentrations of oxyhemoglobin (HbO_2), deoxyhemoglobin (HbR), water (H_2O), and lipid (FAT) are derived[10] from broadband absorption spectra. Unlike conventional near-infrared spectroscopy, broadband DOS directly measures tissue optical scattering, as well as water and lipid concentrations to provide accurate quantification of tissue chromophores. Previous preclinical studies have shown that broadband DOS is sensitive to hemoglobin and StO_2 levels during hemorrhagic shock and transfusion-based resuscitations.[12,13]

In this study, we apply a two-channel broadband DOS instrument to assess tissue hemodynamics in a swine model of severe hemorrhage and REBOA resuscitation. Typical systemic parameters, namely, MAP, SV, and HR, are contrasted with regional DOS parameters.

METHODS

This analysis involved a subset ($N = 17$) of male Sinclair miniature swine (Sinclair Bio Resources, MO, USA), weighing 37 ± 7 kg, involved in a larger ($N = 35$) study of massive hemorrhage and resuscitation.[3] Seven subjects were excluded due to low signal-to-noise ratio (SNR) ($N = 3$), absent data at critical time points such as baseline ($N = 2$), and unusually low baseline HbO_2 values below 1 μM ($N = 2$), resulting in 10 analyzable subjects. Low SNR and total hemoglobin values were likely due to variations in probe placement on Sinclair swine, which have thick avascular subcutaneous tissue. The study was approved by the U.S. Army Institute of Surgical Research Animal Care and Use Committee (protocol number A-14-002). It was conducted in compliance with the Animal Welfare Act and the implementing Animal Welfare Regulations and in accordance with the principles of the "Guide for the Care and Use of Laboratory Animals." It was performed at a facility accredited by AAALAC International.

Surgical procedures are described in greater detail in Park et al.[3] Briefly, the swine were anesthetized and then monitored using an anesthesia machine (Dräger Fabius GS, Dräger Medical Inc., PA, USA). The animal was then placed in a custom sling, allowing it to rest in an anatomic quadruped position. Controlled hemorrhage was achieved using a programmable peristaltic pump (Masterflex, Cole-Parmer, IL, USA). Blood was recovered from the animal into blood collection bags. The blood collection bags rested on a digital scale in order to provide a metric on the amount of fluid removed. The hemorrhage consisted of 65% total blood volume (TBV) hemorrhage over 60 min, where TBV was estimated as 65 mL/kg. The hemorrhage rate was approximately exponential, with the target values listed in Table I.

After the hemorrhage period, the peristaltic pump was stopped. Immediately following, the REBOA device was introduced via the common femoral artery and placed between the subclavian and the celiac arteries (aortic zone 1).[9] The endovascular device utilized was an investigational catheter (ER-REBOA, Pryor Medical, Inc., TX, USA) designed specifically for REBOA applications. After device placement, the balloon was inflated for 30 min using 8 mL of saline solution. Successful occlusion was confirmed by arterial blood pressure dropping to near 0 downstream from the occlusion. Balloon placement was also verified after the experiment by computed tomography and necropsy. A high-pressure monitoring line (Smith Medical ASD INC., OH, USA) was used with an Infinity HemoMed Pod (Dräger Medical Inc., Schleswig-Holstein, Germany) for arterial blood pressure measurements. An EKG device (Osypka Medical Inc., CA, USA) was used to record heart rate. Sensor data were averaged over 6 min.

TABLE I. Targeted Blood Loss Volumes for the Controlled Hemorrhage Period. Blood Was Drawn from Each Animal Using a Peristaltic Pump.

Time (min)	Total Blood Volume Hemorrhaged (%)
7.5	13
19	26
31	39
44	52
60	65

By 60 min, approximately 65% of total blood volume was removed from each subject.

Optical measurements were collected with a broadband, dual-channel DOS research device (Beckman Laser Institute, University of California, Irvine, CA, USA). A custom plastic fiber-coupled probe with a source detector separation distance of 20 mm was secured to the neck (DOS channel 1) and ham (DOS channel 2) of the subjects using sutures, as shown in Figure 1. Measurements were taken approximately every 15 s, and 6-min block averages are presented in this report.

The technology behind the DOS instrument has been extensively detailed in previous studies.[10,11,14] Briefly, the device contains a frequency domain photon migration (FDPM) component consisting of four discrete wavelength sources (660, 690, 785, and 830 nm laser diodes, 20 mW average optical power) and an avalanche photodiode module (C5658 module with S6045-03 photodetector, Hamamatsu, Japan). The broadband steady-state component consists of a tungsten-halogen broadband source (Ocean Optics HL-2000, FL, USA) and spectrometer (AvaSpec-ULS2048X64-USB2, Apeldoorn, the Netherlands). Fiber bundles deliver and collect the light to/from the tissue. After calibration by use of a reference optical phantom, the FDPM amplitude and phase are fit using the P_1 diffusion approximation to the radiative transport equation in order to recover the absorption (μ_a) and reduced scattering (μ_s') coefficients for each laser diode wavelength.[15,16] The broadband state–state reflectance spectrum is calibrated with a reflectance standard (Labsphere Inc., NH, USA). The μ_s' is recovered across the near-infrared wavelength range by fitting μ_s' values from the FDPM component of the DOS device to a power law,

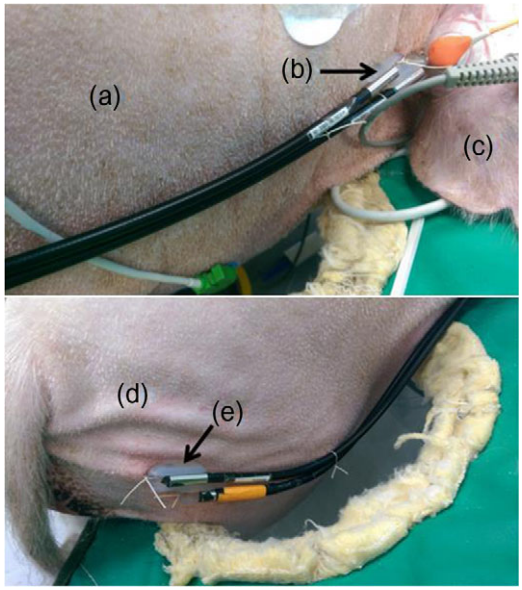

FIGURE 1. Location of the measurement sites shown: (a) neck; (b) broadband diffuse optical spectroscopy (DOS) channel 1 probe; (c) ear; (d) ham; (e) DOS channel 2 probe.

$\mu_s'(\lambda) = A\lambda^{-B}$, in which A is the scatter amplitude, λ is the wavelength, and B is the scattering slope.[10,17,18]

Total data-acquisition time including both the frequency domain and steady-state component is typically under 5 s. Chromophore concentrations are calculated by performing a least-squares minimization including HbO_2, HbR, H_2O, and FAT to the broadband near-infrared absorption spectrum. In addition, a spectrally flat baseline offset was included in the fit, which has been shown to improve the chromophore fits for broadband DOS devices.[19] Additional indices are derived from these parameters, including total hemoglobin (THC = HbO_2 + HbR) and StO_2.

Because of the correlation in the percentage change from baseline across measurement times, generalized estimating equation (GEE) analyses were performed for DOS parameters, with a normal link function and an exchangeable working matrix. From GEE models, the estimated mean and standard error of the percentage change from baseline was obtained and used to construct scatter plots.

Linear regression analysis was performed in which the data for the 10 subjects were averaged for each time point. The mean and standard error for baseline DOS parameters were calculated for each channel. The coefficient of determination (R^2) and p-value was estimated using the MATLAB "corr" function as a measure of the linear relationship between DOS and systemic parameters.

RESULTS

Baseline DOS parameters for each channel before hemorrhage are shown in Table II. Recovered "A" and "B" parameters from the scattering power law in equation (1) are also provided. We note the relatively low StO_2 at these tissue sites in the Sinclair model, likely due to the relatively low perfusion and total hemoglobin content in their thick fatty subcutaneous tissue (HbO_2 = 7 and 8 μM, FAT% = 33 and 45; neck and ham, respectively).

TABLE II. Tabulated Absolute Quantities from Neck (Channel 1) and Ham (Channel 2) of the Diffuse Optical Spectroscopy Instrument at Baseline Are Shown. Recovered "A" and "B" Parameters from the Scattering Power Law in Equation (1) Are Also Provided.

Parameter	Neck	Ham
HbO_2 (μM)	6.7 ± 1.8	7.8 ± 2.4
HbR (μM)	10.1 ± 0.9	11.2 ± 0.8
StO_2 (%)	36.3 ± 5.8	35.7 ± 7.0
THC (μM)	16.6 ± 1.6	18.7 ± 2.3
H_2O (%)	50.0 ± 1.2	51.3 ± 3.7
FAT (%)	32.7 ± 2.7	45.2 ± 2.8
Scattering parameter A	2.1 ± 0.1	2.1 ± 0.3
Scattering parameter B	−1.6 ± 0.1	−1.6 ± 0.2

The baseline for each subject was defined as a 6-min average before the start of hemorrhage. Errors are reported as standard error. (*Note.* HbO_2, oxyhemoglobin; HbR, deoxyhemoglobin; StO_2, hemoglobin oxygenation saturation; THC, total hemoglobin; H_2O, water; FAT, lipid).

Time-varying DOS parameters and standard cardiac measures (MAP, HR, and SV) from the GEE model during hemorrhage and REBOA are shown in Figure 2. Because of subject-to-subject variation in baseline DOS values, the data are presented as percent change from baseline values. The total experiment duration was 90 min, described by three major events: baseline at 0 min, hemorrhage until 60-min mark, and REBOA between the 60- and 90-min marks. For all subjects, channel 1 measured upstream from the occlusion (neck), whereas channel 2 measured downstream (ham).

Hemodynamic trends are shown in Figure 2A. The mean difference between the two DOS channels was calculated using a GEE model. Red asterisks are used to denote when the difference between channels was statistically significant (i.e., the 95% confidence interval of the mean differences did not cross the zero value). In both measurement sites, HbO_2 and StO_2, which are reflective of tissue microvascular perfusion and metabolism, respectively, decreased during hemorrhage, whereas HbR increased. This is consistent with increased oxygen extraction accompanying diminished perfusion during hemorrhage. The HbR increased rapidly in the ham region and then leveled off to match the change in the neck region by the end of the hemorrhage period. During REBOA, HbO_2 increased in the neck, whereas it continued to decrease in the ham. The HbR increased significantly in the ham during REBOA from minutes 72 until 84. By the end of the REBOA, HbO_2, HbR, and StO_2 in both channels converged and no longer remained significantly different.

In Figure 2B, bulk tissue H_2O, FAT, and THC trends are displayed. For the majority of the experiment, H_2O, FAT, and THC remained within a few percent from baseline. No significant difference was observed between channels for

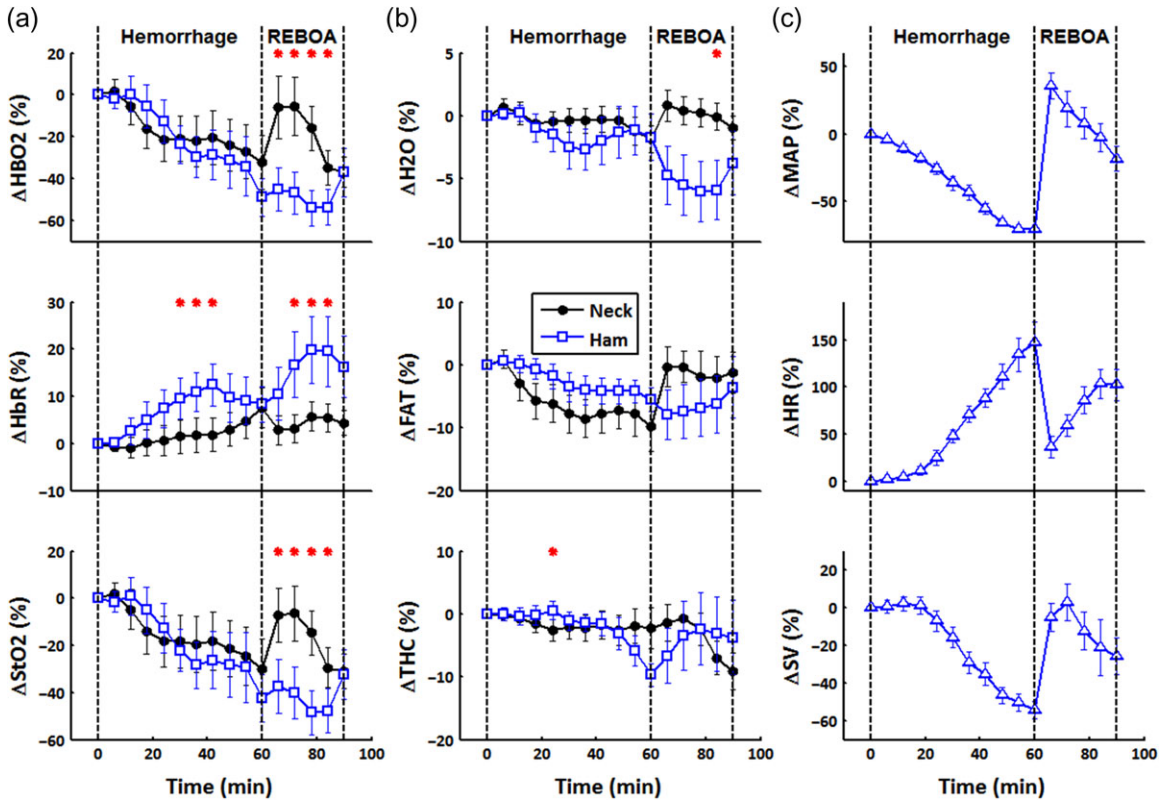

FIGURE 2. Diffuse optical spectroscopy (DOS) and cardiac parameters from a generalized estimating equations model over time. Hemorrhage occurred from 0 to 60 min followed by REBOA at 60–90 min. For all animals, channel 1 measured upstream from the aortic occlusion site (neck), whereas channel 2 measured downstream (ham). Each time point is an average of 6 min of data and is presented as the percent change from its baseline value. Significant difference between channels is denoted by a red asterisk (*). (a) Hemodynamic trends HbO_2, HbR, and StO_2 from the dual-channel DOS device. (b) H_2O, FAT, and THC tissue parameters from the dual-channel DOS device. (c) MAP, HR, and SV systemic parameters from various clinical instruments. (*Note*. HbO2, oxyhemoglobin; HbR, deoxyhemoglobin; StO_2, hemoglobin oxygenation saturation; THC, total hemoglobin; H_2O, water; FAT, lipid; MAP, mean arterial pressure; HR, heart rate; SV, stroke volume).

most time points. However, broadband DOS characterization of H_2O and FAT composition played an important role in the ability of DOS to accurately assess hemodynamics due to the relatively high fat and low hemoglobin levels in the skin of the Sinclair swine model.

Typical cardiac parameters are shown in Figure 2C. During hemorrhage, MAP and SV deteriorated, whereas HR increased. During REBOA, MAP and SV exhibited a sudden increase after inflation of the aortic balloon. However, as the aortic balloon remained inflated, MAP and SV began to decrease below baseline values, but stayed above end-hemorrhage levels. Heart rate responded in similar but opposite trends, showing a decline soon after REBOA inflation, but increased as REBOA was maintained.

Linear regression analysis was performed comparing HbO_2 with MAP and SV as shown in Figure 3A and B for the neck and ham region, respectively. Data for the 10 subjects were averaged at each time point for each channel. Coefficients of determination (R^2) and p-values characterizing the linear relationship between DOS and cardiac parameters were calculated. During the hemorrhage, HbO_2 was strongly associated with MAP in neck ($R^2 = 0.76$, $p = 0.001$) as well as ham regions ($R^2 = 0.89$, $p < 0.001$). During REBOA, neck HbO_2 remained correlated with MAP ($R^2 = 0.83$, $p = 0.03$), whereas ham HbO_2 was no longer associated ($R^2 = 0.06$, $p = 0.70$). Similar associations observed between HbO_2 and SV. The HbO_2 and SV were correlated in both measurement sites during hemorrhage (neck $R^2 = 0.65$, $p = 0.01$; ham $R^2 = 0.90$, $p < 0.001$), but only in neck during REBOA (neck: $R^2 = 0.92$, $p = 0.01$; ham: $R^2 = 0.03$, $p = 0.77$).

Table III further details the coefficients of determination relating DOS and cardiac parameters. During hemorrhage, all DOS parameters are associated ($p < 0.05$) with cardiac parameters in both channels. During REBOA, HbO_2 and StO_2 remained associated with all systemic parameters in channel 1. For channel 2, no associations with cardiac parameters were observed.

DISCUSSION

There has been much interest in assessing the potential of REBOA to replace thoracotomy with aortic clamping as a minimally invasive approach to treat non-compressible hemorrhage.[1–7] In previous work, we were able to assess the

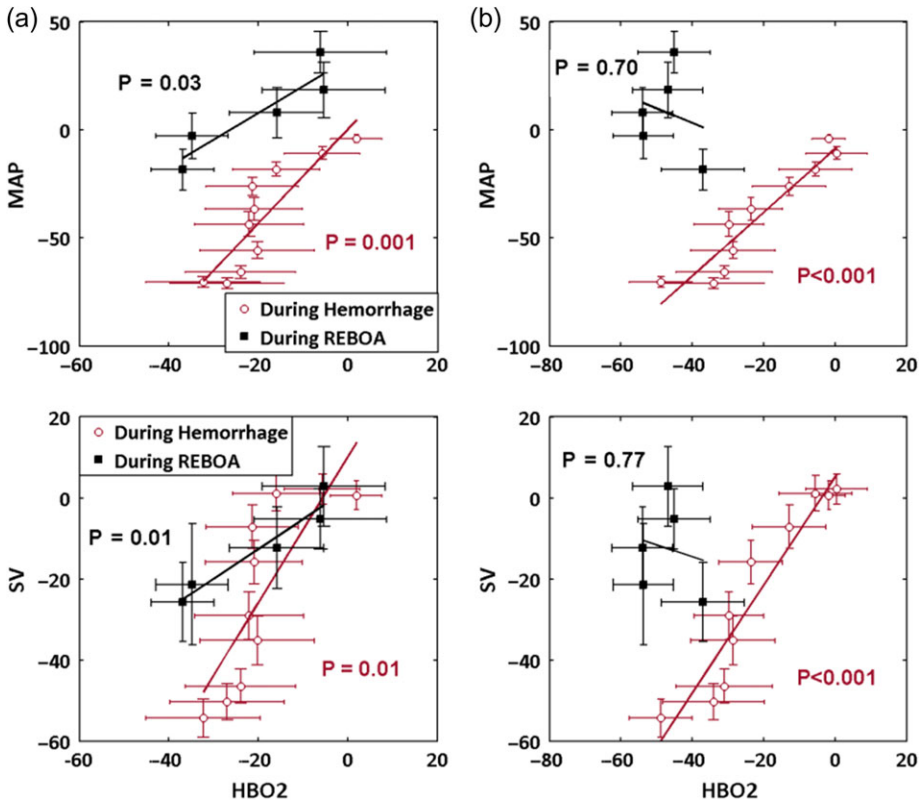

FIGURE 3. Linear regression analysis of HbO_2 with systemic parameters SV and MAP. (a) Neck HbO_2 is significantly associated with MAP and SV during the hemorrhage and maintains significance during REBOA. (b) Ham HbO_2 is highly correlated with MAP and SV during hemorrhage, but loses significant association during REBOA. (*Note*. HbO_2, oxyhemoglobin; MAP, mean arterial pressure; SV, stroke volume).

TABLE III. Diffuse Optical Spectroscopy (DOS) Channel 1 (Top) and Channel 2 (Bottom) Coefficients of Determination for All 10 Subjects.

	Hemorrhage			REBOA		
	MAP	HR	SV	MAP	HR	SV
	Channel 1 Coefficients of Determination (R^2)					
HbO_2	0.76*	0.69*	0.65*	0.83*	0.82*	**0.92***
HbR	0.79*	0.88*	0.82*	0.40	0.69	0.43
StO_2	0.79*	0.72*	0.68*	0.82*	0.82*	**0.92***
	Channel 2 Coefficients of Determination (R^2)					
HbO_2	0.89*	**0.91***	**0.90***	0.06	0.01	0.03
HbR	0.61*	0.46*	0.49*	0.38	0.62	0.14
StO_2	0.88*	0.88*	0.88*	0.01	0.06	0.00

During REBOA, DOS parameters in channel 1 associate with systemic parameters, whereas channel 2 is not. The asterisk (*) is used to denote if the relationship is statistically significant ($p < 0.05$). Cases with high coefficients of determination ($R^2 > 0.90$) are displayed as bold text. (*Note*. HbO_2, oxyhemoglobin; HbR, deoxyhemoglobin; StO_2, hemoglobin oxygenation saturation; MAP, mean arterial pressure; HR, heart rate; SV, stroke volume).

efficacy of transfusion-based resuscitation using a single-channel DOS that monitored systemic hemoglobin levels with a non-invasive probe.[12,20] However, REBOA necessitates occlusion of the aorta, and thus, the subsequent creation of two distinct blood volume compartments: an upstream compartment and a downstream compartment. Accordingly, in this study, we employ a dual-channel DOS instrument in order to follow regional tissue hemodynamics from two different blood volume compartments in a model of massive hemorrhage and REBOA.

Baseline concentrations of HbO_2, HbR, StO_2, THC, and H_2O were similar at each measurement site, whereas FAT levels were slightly elevated in the ham region. However, because of the thick subcutaneous fat layer of the swine model, we observed relatively high overall FAT% and low THC at baseline. This is consistent with a previous study,[21] which reported a similar adipose composition measured in humans as well as our own observations (data not shown) of resected skin showing up to 2-cm-thick adipose in the ham region. Under these conditions, the ability of broadband DOS utilizing hundreds of optical wavelengths to quantitatively measure all major tissue components can improve sensitivity to hemodynamics during hemorrhage and REBOA.

During the hemorrhage period, the resulting HbO_2, HbR, and StO_2 trends were as expected for a blood loss model: HbO_2 and StO_2 decreased over time, whereas HbR remained elevated from baseline. This is indicative of hemorrhage-induced reductions in microvascular perfusion accompanied by an increase in tissue oxygen extraction. No significant difference was observed between neck and ham in the rate

of HbO_2 and StO_2 decrease during hemorrhage. The values for HbR in the neck were significantly different from the ham for a period of 18 min as seen in Figure 2A. However, by the end of the hemorrhage period, HbR trends in both channels were no longer statistically different. This temporary divergence in HbR may have been the result of initially different metabolic rates of the two underlying tissue sites. Overall, DOS and conventionally measured systemic parameters (MAP, HR, and SV) were significantly correlated in both channels during the hemorrhage period, as shown in Table III. These results indicate that both DOS channels were capable of tracking hemorrhage with similar performance to invasively obtained systemic parameters.

During REBOA, significant differences between DOS channels were observed for HbO_2 and StO_2 between 66 and 84 min as seen in Figure 2A; differences were also observed between 72 and 84 min for HbR. This observation is explained by the fact that the neck channel interrogated an area in which blood pressure was restored as a result of REBOA inflation, whereas the ham channel probed a region in which no intervention was provided. In other words, two blood volume compartments with unique hemodynamics were formed as a direct consequence of the aortic occlusion. Two measurement sites, and thus, two-channel systems, are recommended for investigating REBOA models.

During severe hemorrhage, loss of blood volume leads to a reduction of systemic blood pressure. Under these conditions, HR increases in an attempt to compensate for reduced SV to meet tissue metabolic demands. Throughout the hemorrhage period, DOS parameters in both channels were significantly correlated with systemic parameters as presented in Table III. However, upon REBOA inflation, the DOS channel measuring downstream (ham) from the occlusion loses all association with systemic parameters. This clear discrepancy between systemic and tissue-level assessments suggests that conventional metrics such as MAP, HR, and SV cannot be used to characterize the impact of REBOA on downstream tissue viability. In contrast, as shown in Figure 2A, despite isolation from blood flow, DOS recovers hemodynamics as well as tissue status in this region. Thus, during hemorrhage, two-channel DOS tracks conventional systemic parameters, and during REBOA, DOS can provide additional information, this is not available systemically. One potential application of these findings is studying standard REBOA procedures, such as the length and degree of occlusion. Maximizing survival rates while minimizing harmful physiological consequences of ischemia are desirable but remain challenging.[4,22]

Several limitations can be identified in this study. Although DOS is capable of recovering tissue hemoglobin and oxygenation status, the highly scattering nature of light propagation in skin and the 2-cm source detector separation of our DOS probe limits the mean interrogation depth to ~6–9 mm for typical 2-cm-thick tissues.[23] Although this is sufficient for recovering subsurface microvascular hemodynamics, deeper organ status cannot be evaluated non-invasively. We also utilized Sinclair swine subjects with variably thick, low blood volume, fatty skin. In addition, fiber-coupling inefficiencies with light sources as well as detector components resulted in lower-than-expected DOS signal-to-noise ratios (SNR). Finally, the effect of anesthesia on hemodynamic responses is difficult to quantify.

The results of this study demonstrate the feasibility of a non-invasive, two-channel DOS device to assess hemodynamics in different tissue regions during hemorrhage and REBOA-induced resuscitation. Highly correlated relationships between DOS and systemic parameters were seen during hemorrhage and maintained during REBOA upstream of the aortic occlusion. Downstream of the occlusion, systemic MAP, HR, and SV are uncorrelated with tissue status, whereas DOS maintains sensitivity to regional changes in tissue perfusion and metabolism. We conclude that dual-channel DOS measurements of regional tissue perfusion and metabolism can be used successfully to non-invasively track the formation of hemodynamically distinct tissue compartments during hemorrhage and REBOA resuscitation. As conventional systemic measures (MAP, HR, SV) correlate with DOS upstream of REBOA but do not provide information on downstream tissue status, multi-compartment, non-invasive DOS monitoring may provide a more complete picture of the efficacy of REBOA and similar resuscitation procedures.

CONFLICTS OF INTEREST

Office of the University of California, Irvine, has reviewed both patent and corporate disclosures and did not find any concerns. No potential conflicts of interest were disclosed by the other authors

PRESENTATIONS

Presented as a poster at the 2016 Military Health System Research Symposium (abstract number: MHSRS-16-0801).

FUNDING

This research was supported by AFOSR grant award FA9550-14-1-0034 (Advanced Optical Technologies for Defense Trauma and Critical Care). This research was also supported by National Institutes of Health P41EB015890, the Laser Microbeam and Medical Program (LAMMP), as well as the Arnold and Mabel Beckman Foundation. The animal work was funded by a grant by the Telemedicine and Advanced Technologies Research Center, Fort Detrick, MD, to Pryor Medical, Inc., Arvada, CO, and via a subcontract between Pryor Medical and the Geneva Foundation, Tacoma, WA, for work performed at the U.S. Army Institute of Surgical Research.

REFERENCES

1. Morrison JJ, Ross JD, Houston R, Watson JDB, Sokol KK, Rasmussen TE: Use of resuscitative endovascular balloon occlusion of the aorta in a highly lethal model of noncompressible torso hemorrhage. Shock 2014; 41(2): 130–7.
2. White JM, Cannon JW, Stannard A, Markov NP, Spencer JR, Rasmussen TE: Endovascular balloon occlusion of the aorta is superior to resuscitative thoracotomy with aortic clamping in a porcine model of hemorrhagic shock. Surgery 2011; 150(3): 400–9.
3. Park TS, Batchinsky AI, Belenkiy SM, et al: Resuscitative endovascular balloon occlusion of the aorta (REBOA): comparison with immediate

transfusion following massive hemorrhage in swine. J Trauma Acute Care Surg 2015; 79(6): 930–6.
4. Qasim Z, Brenner M, Menaker J, Scalea T: Resuscitative endovascular balloon occlusion of the aorta. Resuscitation 2015; 96: 275–79.
5. Brenner ML, Moore LJ, DuBose JJ, et al: A clinical series of resuscitative endovascular balloon occlusion of the aorta for hemorrhage control and resuscitation. J Trauma Acute Care Surg 2013; 75(3): 506–11.
6. Markov NP, Percival TJ, Morrison JJ, et al: Physiologic tolerance of descending thoracic aortic balloon occlusion in a swine model of hemorrhagic shock. Surg (United States) 2013; 153(6): 848–56.
7. Avaro J-P, Mardelle V, Roch A, et al: Forty-minute endovascular aortic occlusion increases survival in an experimental model of uncontrolled hemorrhagic shock caused by abdominal trauma. J Trauma Inj Infect. Crit Care 2011; 71(3): 720–6.
8. Ledgerwood A, Kazmers M, Lucas C: The role of thoracic aortic occlusion for massive hemoperitoneum. J Trauma Acute Care Surg 1976; 16 (8): 610–5.
9. Stannard A, Eliason JL, Rasmussen TE: Resuscitative endovascular balloon occlusion of the aorta (REBOA) as an adjunct for hemorrhagic shock. J Trauma Inj Infect. Crit Care 2011; 71(6): 1869–72.
10. Bevilacqua F, Berger AJ, Cerussi AE, Jakubowski D, Tromberg BJ: Broadband absorption spectroscopy in turbid media by combined frequency-domain and steady-state methods. Appl Opt 2000; 39(34): 6498–507.
11. No K-S, Kwong R, Chou PH, Cerussi A: Design and testing of a miniature broadband frequency domain photon migration instrument. J Biomed Opt 2009; 13(5): 50509–1-50509-3.
12. Lee J, Cerussi AE, Saltzman D, Waddington T, Tromberg BJ, Brenner M: Hemoglobin measurement patterns during noninvasive diffuse optical spectroscopy monitoring of hypovolemic shock and fluid replacement. J Biomed Opt 2007; 12: 24001-1–24001-8.
13. Lee J, Kim JG, Mahon S, et al: Broadband diffuse optical spectroscopy assessment of hemorrhage- and hemoglobin-based blood substitute resuscitation. J Biomed Opt 2010; 14(4): 44027-1–44027-7.
14. Cerussi A, Shah N, Hsiang D, Durkin A, Butler J, Tromberg BJ: In vivo absorption, scattering, and physiologic properties of 58 malignant breast tumors determined by broadband diffuse optical spectroscopy. J Biomed Opt 2006; 11(4): 044005-1–044005-16. doi:10.1117/1.2337546.
15. Tromberg BJ, Svaasand LO, Tsay TT, Haskell RC: Properties of photon density waves in multiple-scattering media. Appl Opt 1993; 32(4): 607–16.
16. Pham TH, Coquoz O, Fishkin JB, Anderson E, Tromberg BJ: Broad bandwidth frequency domain instrument for quantitative tissue optical spectroscopy. Rev Sci Instrum 2000; 71(6): 2500–13.
17. Schmitt JM, Kumar G: Optical scattering properties of soft tissue: a discrete particle model. Appl Opt 1998; 37(13): 2788–97.
18. Mourant JR, Fuselier T, Boyer J, Johnson TM, Bigio IJ: Predictions and measurements of scattering and absorption over broad wavelength ranges in tissue phantoms. Appl Opt 1997; 36(4): 949–57.
19. Jakubowski DB: Development of broadband quantitative tissue optical spectroscopy for the non-invasive characterization of breast disease. 2002. http://search.proquest.com/docview/304798175; accessed November 4, 2016.
20. Lee J, Kim JG, Mahon S, et al: Tissue hemoglobin monitoring of progressive central hypovolemia in humans using broadband diffuse optical spectroscopy. J Biomed Opt 2008; 13(6): 1–10.
21. Ganesan G, Warren RV, Leproux A, et al: Diffuse optical spectroscopic imaging of subcutaneous adipose tissue metabolic changes during weight loss. Int J Obes 2016; 40(8): 1292–1300.
22. Russo RM, Williams TK, Grayson JK, et al: Extending the golden hour: partial resuscitative endovascular balloon occlusion of the aorta in a highly lethal swine liver injury model. J Trauma Acute Care Surg 2016; 80(3): 372–80.
23. Yu G, Durduran T, Zhou C, Cheng R, Yodh A: Near-infrared diffuse correlation spectroscopy for assessment of tissue blood flow. In: Handbook of Biomedical Optics, pp 195–216. Boca Raton, FL, CRC Press, 2011.